

## 基于太赫兹超材料的牛血清白蛋白传感器研究

郑卓锐<sup>1,4</sup>, 钟慧<sup>1\*</sup>, 聂勇潇<sup>1,2</sup>, 林婷<sup>1,3</sup>, 方依靠<sup>1</sup>, 宋立伟<sup>1,4</sup>, 田野<sup>1,4</sup><sup>1</sup>中国科学院上海光学精密机械研究所强场激光物理国家重点实验室, 上海 201800;<sup>2</sup>华中科技大学光学与电子信息学院, 湖北 武汉 430074;<sup>3</sup>上海理工大学光电信息与计算机工程学院, 上海 200093;<sup>4</sup>中国科学院大学材料与光电研究中心, 北京 100049

**摘要** 太赫兹波具有非电离、对非极性物质穿透性高、对氢键等弱共振敏感等特性,是生物、材料、化学等领域的重要研究对象。蛋白质、糖类等生物大分子的转动频率和基团的振动频率以及分子之间弱相互作用的特征频率恰好处于太赫兹频段,这赋予了太赫兹光谱技术在生物医学领域中极大的发展潜力。然而,由于待测物尺寸一般小于太赫兹波长(0.03~3.00 mm),微量的待测物难以引起谱线的改变,太赫兹光谱检测灵敏度较低。能够灵活操控电磁波特性的超材料为解决上述问题提供了新的思路,通过设计不同的结构及参数,能够得到谐振频率位于太赫兹波段的超材料,微量的待测物即可引起谱线的明显变化。基于共振型太赫兹超材料构建了牛血清白蛋白(BSA)传感器,实验结果表明,当BSA溶液的体积质量为2.0~8.0 mg/mL时,传感器共振频率偏移量与溶液浓度呈线性关系,传感器的最低浓度检测限为0.3 mg/mL。

**关键词** 光谱学; 太赫兹; 超材料; 牛血清白蛋白; 传感器

中图分类号 O436 文献标志码 A

DOI: 10.3788/CJL230881

## 1 引言

0.1~10.0 THz 频段间的电磁波被称为太赫兹波、亚毫米波,其波谱位于微波和红外辐射之间<sup>[1]</sup>。相较于其他波段,太赫兹波具有很多重要的特性,它的带宽较宽,具有很强的穿透性,辐射的光子能量较低,其光子能量与生物大分子的旋转能级和振动能级处于同一量级<sup>[2]</sup>。此外,分子间弱相互作用(氢键、范德瓦耳斯力等)、大分子骨架振动等恰好发生在太赫兹波段<sup>[2-5]</sup>。在生物医学研究领域,太赫兹检测有着得天独厚的优势:太赫兹波段对弱共振十分敏感,太赫兹波的频率范围与许多重要生物大分子(蛋白质、糖类和核酸等)的振动频率相关<sup>[6]</sup>。此外,太赫兹波具有非侵入性、非接触、非电离辐射式及生物友好性<sup>[7]</sup>。

由于具备上述突出优点,太赫兹波已被用于研究生物分子的特性(如分子结构)及分子与周围环境的相互作用等。Yoneyama等<sup>[8-9]</sup>设计了一种可承载蛋白质样品的膜结构,并结合太赫兹时域光谱仪,对牛血清白蛋白(BSA)的天然构象和热变性构象进行测定,结果表明两种样品在透光率和相位上有明显的差异,证明

了太赫兹光谱技术在研究和鉴别蛋白质分子构象方面的可行性。Cheon等<sup>[10]</sup>对癌症脱氧核糖核酸(DNA)甲基化的太赫兹指纹谱进行研究,结果表明太赫兹波可与DNA中甲基化的分子共振,直接观测到DNA的变化,即利用癌症DNA在太赫兹频段内的甲基化信号,可以对正常DNA和癌症DNA进行区分。在传统的生物检测技术中,标记是一个难以避免的步骤,如添加特异性抗体、荧光素等,然而此类生物标签的使用不仅会降低检测效率,还可能对实验样品的分子构象造成影响。利用太赫兹时域光谱仪系统,Han等<sup>[11]</sup>利用太赫兹透射谱提取出样品折射率,实现了在无标记的情况下对不同种蛋白质溶液的检测与区分。

由于太赫兹波的波长(0.03~3.00 mm)与常见的生物大分子等待测样品的特征尺寸不在同一量级,如蛋白质颗粒、病毒的直径一般是纳米量级,在实际非破坏性检测中,样品所含的微量生物大分子与太赫兹波之间难以发生充分的相互作用,太赫兹谱线的微弱变化难以被捕捉到<sup>[7]</sup>。上述问题使得太赫兹光谱检测技术的灵敏度较低,极大地阻碍了其在各领域中的应用和发展。超材料是一种由亚波长结构按照一定规则排

收稿日期: 2023-06-01; 修回日期: 2023-07-24; 录用日期: 2023-08-01; 网络首发日期: 2023-08-11

基金项目: 国家自然科学基金(62105346)、科技部重点研发专项(2022YFA1604400)、基础研究特区计划(JCYJ-SHFY-2021-002)、中国科学院基础前沿科学研究计划(ZDBS-LY-SLH018)、中国科学院青年促进会项目、强场激光物理国家重点实验室开放课题

通信作者: \*zhonghui@siom.ac.cn

列的人工材料,其具有天然材料所不具备的强大的电磁波操控能力,科研人员已经利用超材料实现了许多新颖的功能及特性,例如负折射率、异常偏折、波长选择性吸收和电磁感应透明(EIT)等<sup>[12-16]</sup>。特别地,通过设计特定的结构可以获得具有共振功能的超材料,在共振频点处,入射的电磁波被局域化并得到极大的增强,利用该强场能够有效加强物质与电磁波间的相互作用<sup>[17]</sup>。将超材料与太赫兹光谱技术结合,微量甚至痕量水平的待测物给超材料表面带来的微小扰动即可引起超材料谱线(如谐振频点)的可观变化,进而实现对生物大分子的高灵敏度检测<sup>[18]</sup>。

Yang等<sup>[19]</sup>提出了一种开口谐振环(SRR)传感器,利用超材料谐振频率与介电环境的对应关系,实现了野生型和转基因基因组DNA之间的高效无标记区分。王庆芳等<sup>[20]</sup>设计了一种超材料芯片,以7-甲基鸟嘌呤为例,将其最小检测限度从2.95 mg降低到6.30  $\mu\text{g}$ ,从而满足了低浓度检测的应用需求。Lin等<sup>[21]</sup>提出了一种采用抗体修饰的太赫兹生物传感器,利用折射率变化引起的共振频率偏移检测癌胚抗原(CEA)的浓度,结果表明,当抗体体积质量为20 ng/mL时,共振频率偏移量随CEA浓度线性增加。Li等<sup>[22]</sup>基于四个谐振频率相同的电感-电容(LC)共振器设计了牛血清白蛋白传感器,实验表明,随着蛋白质溶液浓度的提高,共振频率出现了明显的红移。在病毒传感检测研究方面,Keshavarz等<sup>[23]</sup>利用太赫兹超材料对不同禽流感病毒(AI)亚型在太赫兹频率范围内的复折射率进行了探究。Park等<sup>[24]</sup>基于LC共振型超材料实现了对典型的双链DNA病毒PRD1(直径为60 nm)和单链核糖核酸(RNA)病毒MS2(直径为30 nm)的低浓度分类检测。Lee等<sup>[25]</sup>利用纳米狭缝式共振芯片,通过太赫兹光谱学研究了0.2~2.0 THz频率范围内三种类型(H1N1、H5N2和H9N2)禽流感病毒的透射谱特性。结果表明,在共振频率的峰值处,太赫兹透射率与样品浓度存在较好的线性关系,并且对于不同类型的禽流感病毒,太赫兹共振频率的频移不同,即表现出病毒特异性。

生物传感与检测一直是一个重要的研究领域,在降低成本的同时,实现快速且可靠的检测一直是其追求目标。目前常用的检测方法,如聚合酶链反应(PCR)<sup>[26]</sup>、酶联免疫吸附法(ELISA)<sup>[27]</sup>和质谱法(MS)<sup>[28]</sup>等,检测时间较长且实验步骤复杂,难以满足快速检测需求。结合超材料与太赫兹光谱技术可以有效避免上述问题。本文利用共振型太赫兹超材料加强太赫兹波与待测物之间的相互作用,选用牛血清白蛋白溶液作为分析物,结合太赫兹光谱技术,构建了高效的牛血清白蛋白传感器。

## 2 数值模拟与实验

太赫兹超材料的单共振或多共振性质主要取决于

单元的独特几何形状和衬底折射率,其共振频率可能会由于周围介质环境的改变而发生偏移(红移或蓝移)。太赫兹超材料一般通过改变传感器表面的待测物,即改变折射率的数值,实现共振频率改变的效果,因此对周围物质的介电常数/折射率变化的敏感度直接决定传感器的性能。

### 2.1 超材料传感性能

描述超材料传感性能的指标一般为质量因子(Q)、灵敏度(S)和品质因数(FoM)值。质量因子Q表示共振倾角的锐度,影响频移的鉴别。理论表明,质量因子数值越大,意味着传感器性能越好。其对传感器的性能起到决定性的作用,表达式为

$$Q = \frac{F_0}{\Delta F}, \quad (1)$$

式中: $F_0$ 为共振频率处的中心频率; $\Delta F = \frac{|F_2 - F_1|}{2}$ ,其中 $F_1$ 和 $F_2$ 分别为光谱曲线最大值的1/2处对应的两个频率。

灵敏度S是单位折射率变化范围内共振频率的偏移量,其表达式为

$$S = \frac{\Delta f}{\Delta n}, \quad (2)$$

式中: $\Delta f$ 为折射率变化引起的共振频率的偏移量; $\Delta n$ 为生物样本折射率( $n$ )的变化量。灵敏度单位为GHz/RIU。

此外,FoM值也是考察共振芯片性能的重要指标之一,它考虑了带宽的影响,可以用于传感器之间性能的比较,其计算方法为

$$F_{\text{FoM}} = S/F_{\text{FWHM}}, \quad (3)$$

式中: $F_{\text{FoM}}$ 为FoM值; $F_{\text{FWHM}}$ 为光谱曲线的半峰全宽(FWHM)。由定义可知FoM值无量纲。当超材料传感器的灵敏度一定时,共振频段的FWHM越小,FoM值越高,传感性能也越好。

### 2.2 超材料结构与数值模拟

为了实现对牛血清白蛋白溶液的快速高灵敏检测,本文采用Sengupta等<sup>[29]</sup>设计的单元结构。由于结构的C4对称性,基于该超材料的传感器对偏振不敏感。当电磁波垂直入射到该结构上时,感应电流的产生引入了等效电感 $L$ ,而开口处由于大量电荷的聚集而形成了等效电容 $C$ ,则LC共振芯片的电磁共振频率可表示为

$$f = \frac{1}{2\pi\sqrt{LC}}. \quad (4)$$

本文所用超材料是由常规微纳工艺加工的,实物显微图如图1中插图所示,整体的大小为6 mm $\times$ 6 mm,衬底为725  $\mu\text{m}$ 厚的单晶硅,在衬底上方沉积了200 nm厚的铝膜,并刻蚀超材料的单元结构。常用的太赫兹超材料大多是偏振相关的。基于传统的LC共振结构,通过将电容器间隙放置在方形传感器的两个

几何对角线上,这种交叉型结构可以在 S 和 P 偏振态下实现偏振无关检测。

对超材料的电磁特性进行全波数值仿真,由模拟

结果可知,上述结构在 0.8 THz 附近存在共振吸收。通过改变超材料金属结构的折射率,超材料的共振峰出现了频率偏移现象。

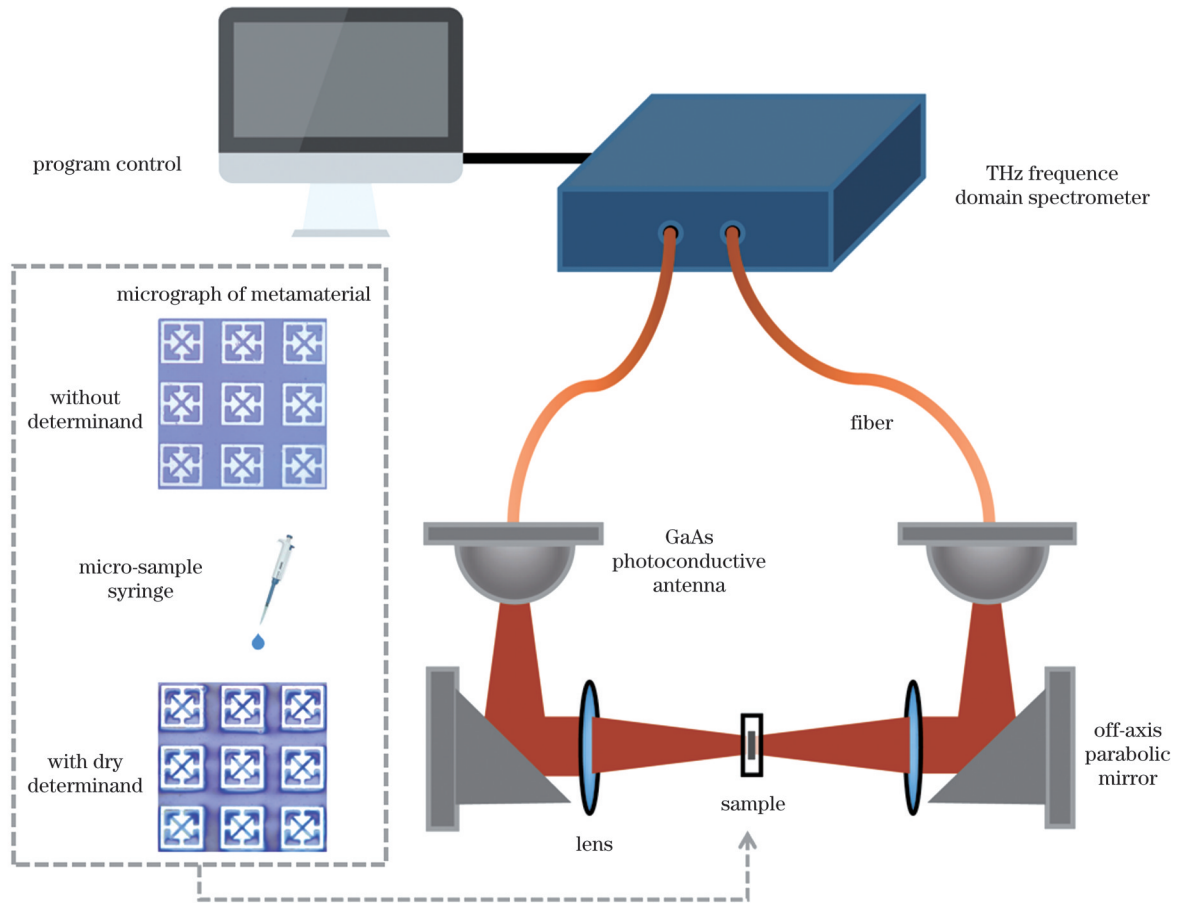


图 1 实验装置示意图,其中插图为未滴加待测物及滴加待测物并烘干后的超材料显微照片

Fig. 1 Schematic of experimental set up with micrographs of metamaterials without determinand and with dry determinand shown in inset

### 2.3 实验设计

为了对所加工超材料的传感特性进行检验,选用牛血清白蛋白作为待测物,结合太赫兹光谱仪进行太赫兹透射测量实验,实验装置如图 1 所示。GaAs 光电导天线将特定频率的太赫兹电磁波辐射至离轴抛物面镜,离轴抛物面镜将太赫兹波以平面波形式反射至聚焦透镜,太赫兹波被聚焦至超材料样品表面,太赫兹波透过样品后依次经过透镜及离轴抛物面镜,被 GaAs 光电导天线接收。计算机控制太赫兹频谱仪的参数,并对实验数据进行分析处理。采用牛血清白蛋白作为待测物是因为其是牛肝细胞合成的,是牛血清中主要的、常用的载体蛋白,具有重要的运输和存储功能。此外,其易溶于水,具有良好的热稳定性,在生化实验中有着广泛的应用。

为了使超材料垂直放置于测试光路中,本文设计并制作了高聚乙烯(HDPE)材质的夹持装置。在实验过程中,超材料被夹持装置固定于光路中。首先利用太赫兹光谱仪测得超材料上无待测物时的透射光谱数据,并以其作为背景组。然后,取定量牛血清白蛋白样

品溶于蒸馏水中,制备一定浓度的牛血清白蛋白溶液作为待测溶液,通过微量进样器取 20  $\mu\text{L}$  待测溶液,滴于超材料上,将其置于 70  $^{\circ}\text{C}$  的加热台上加热 10 min。如图 1 插图所示,烘干后待测的牛血清白蛋白完全覆盖在超材料表面上。通过太赫兹光谱仪对超材料的透射光谱进行测量,将其作为样品组。在实验过程中,为了减小误差,对单次扫描相邻点的数据进行线性加权平均处理;每个样品的最终数据为三次扫描结果的平均值。

### 3 分析与讨论

在实验过程中,采用太赫兹光谱仪测得 HDPE 夹持装置未夹持超材料时的太赫兹透射谱线。进一步地,采用 HDPE 夹持装置固定未滴加待测物的超材料,测得其太赫兹透射谱线。如图 2 所示,裸芯片的透射谱在 0.8 THz 附近出现了明显的凹陷,表明超材料在该波段处存在一个较强的吸收。由实验数据计算得到该超材料的品质因子  $Q$  值为 26.08。

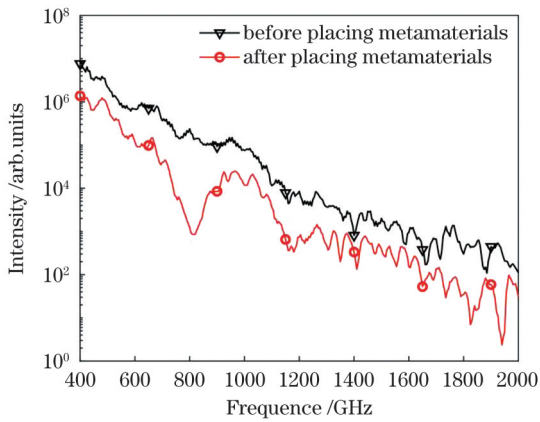


图 2 光路中放置超材料前后的透射谱线

Fig. 2 Transmission spectra before and after placing metamaterials in optical path

为了进一步研究超材料作为生物大分子传感器对牛血清白蛋白的传感特性,将太赫兹光谱仪的扫描范围缩短为 770~840 GHz,采样步长设定为 200 MHz,在超材料表面滴加 20  $\mu$ L 体积质量为 2 mg/mL 的牛血清白蛋白溶液,待其干燥后,再次用光谱仪测量其透射谱。结果表明,添加待测物后,超材料共振频率会往低频的方向移动,如图 3(a)所示。引起上述现象的原因如下:待测物的加入改变了超材料表面的折射率,超材料的共振频率发生了变化。为了分析对比样品组和背

景组两者之间的共振频率偏移情况,采用二阶高斯拟合的方式对两种情况下测得的透射谱线进行非线性拟合,通过对拟合后曲线进行分析,计算其共振频率的偏移量。其中所用的二阶高斯拟合公式为

$$y = a_1 \times \exp(x - b_1)/c_1^2 + a_2 \times \exp(x - b_2)/c_2^2, (5)$$

式中: $a_i, b_i, c_i (i=1, 2)$  为待定的拟合系数; $x$  为自变量; $y$  为因变量。由拟合结果可知,体积质量为 2 mg/mL 的牛血清白蛋白溶液引起超材料的共振频率中心红移 10.43 GHz。利用控制变量法,配置了多组不同体积质量(2、3、4、8 mg/mL)的待测溶液,分别测量其在夹持装置下的太赫兹透射光谱数据,与裸芯片的透射光谱数据进行比较,结果如图 3 所示,对应拟合曲线的共振频率、频移量如表 1 所示。可以看出,随着溶液体积质量的逐步提升,超材料的共振频率逐步向低频方向移动。需要说明的是,实际测试环境的变化、加工误差造成芯片尺寸间存在一定差异,加上人为操作等因素,所得背景曲线存在一定抖动。图 4 为共振频移量与待测溶液体积质量的关系曲线,可见当体积质量在 2~8 mg/mL 范围内时,共振频率偏移量与待测物体体积质量呈线性关系,体积质量的提高使得共振频率的偏移量增大。因此,可以通过测量并分析超材料表面待测物在太赫兹波段透射谱的共振偏移量,得到待测溶液中牛血清白蛋白的体积质量。

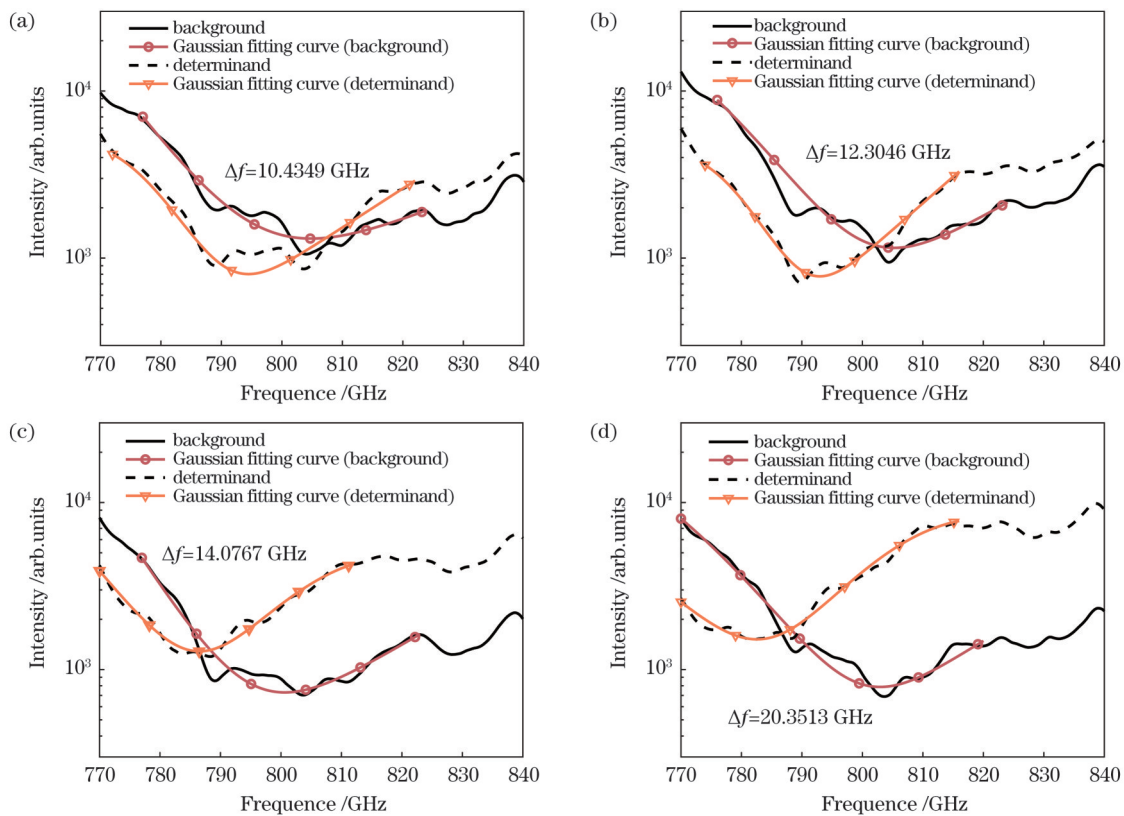


图 3 不同待测物体积质量下的透过率曲线及相应的高斯拟合曲线。(a) 2 mg/mL; (b) 3 mg/mL; (c) 4 mg/mL; (d) 8 mg/mL

Fig. 3 Transmittance curves and corresponding Gaussian fitting curves under different volume mass values of determinands.

(a) 2 mg/mL; (b) 3 mg/mL; (c) 4 mg/mL; (d) 8 mg/mL.

表 1 不同待测物体积质量下的共振频率及频率偏移量

Table 1 Resonance frequencies and frequency offsets under different volume mass values of determinands

Volume mass / ( $\text{mg} \cdot \text{mL}^{-1}$ )	Resonance peak without determinand /GHz	Resonance peak with determinand /GHz	$\Delta f$ /GHz
2	804.8798	794.4449	10.4349
3	805.2425	792.9379	12.3046
4	800.5992	786.5225	14.0767
8	802.9098	782.5585	20.3513

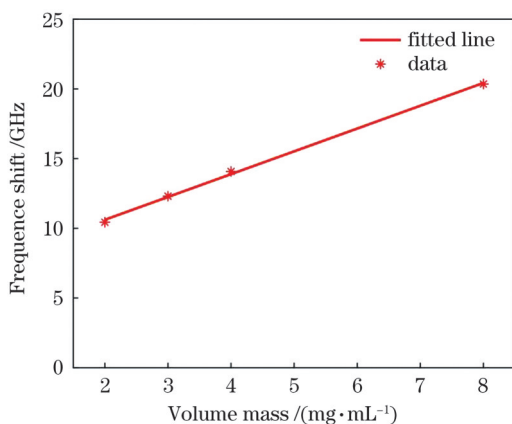


图 4 传感器共振频率偏移量随待测物体积质量的变化曲线  
Fig. 4 Sensor resonance frequency offset versus volume mass of determinand

进一步降低待测溶液体积质量,发现当牛血清白蛋白溶液体积质量为  $1.0 \text{ mg/mL}$  时,共振频移量迅速下降,仅为  $2.0 \text{ GHz}$ ,如图 5(a)所示。这是因为在低体积质量的情况下,由于芯片表面沉积的样品厚度特别薄,受厚度的影响,其共振频率偏移量较小。由此可见,将该超材料与太赫兹光谱技术结合进行生物分子检测时灵敏度较高,即使在低体积质量、折射率改变较小的情况下,也能检测到其共振频率向低频方向的移动。此外,最低浓度检测限对于超材料的性能表征也十分重要。通过进一步配置更低浓度的溶液,重复上述实验,研究低浓度溶液引起的共振频率偏移量,得到该超材料对牛血清白蛋白溶液的最低浓度检测限。由太赫兹透射谱的高斯拟合可见,当体积质量降低到  $0.3 \text{ mg/mL}$  时,共振芯片的频率偏移量为  $0.87 \text{ GHz}$ ,如图 5(b)所示。当体积质量进一步降低到  $0.2 \text{ mg/mL}$  时,共振偏移量不到  $0.04 \text{ GHz}$ ,如图 5(c)所示。三种体积质量下对应拟合曲线的共振频率和频移量如表 2 所示。由于光谱仪的采样步长为  $200 \text{ MHz}$ ,而当溶液的体积质量为  $0.2 \text{ mg/mL}$  时,其共振偏移量仅为采样步长的  $1/5$ 。因此,该系统可以实现低浓度溶液的高灵敏度检测,其最低浓度检测限为  $0.3 \text{ mg/mL}$ 。

利用水溶解蛋白质时会发生水合现象,即会有一层水分子包裹蛋白质分子。在实验过程中采用加热的方式烘干待测溶液,该方式只能去除待测溶液中的自由水,但牛血清白蛋白分子表面的水合层依然存在。由于水对太赫兹波具有强烈的吸收作用,故太赫

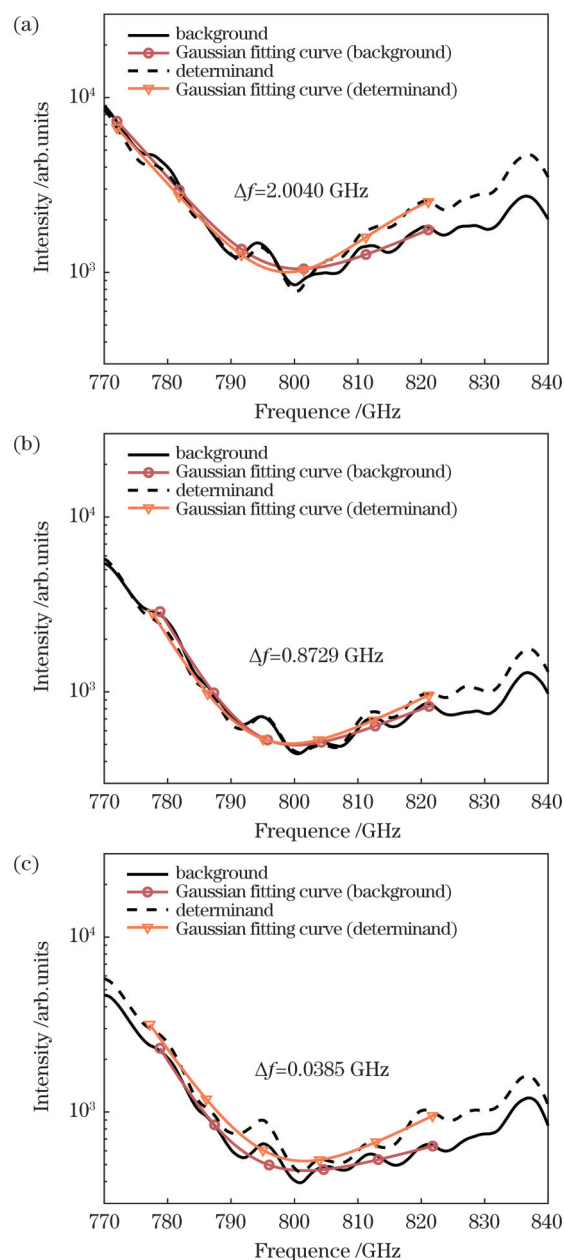


图 5 不同待测物体积质量下的透过率曲线及相应的高斯拟合曲线。(a)  $1.0 \text{ mg/mL}$ ; (b)  $0.3 \text{ mg/mL}$ ; (c)  $0.2 \text{ mg/mL}$   
Fig. 5 Transmittance curves and corresponding Gaussian fitting curves under different volume mass values of determinands. (a)  $1.0 \text{ mg/mL}$ ; (b)  $0.3 \text{ mg/mL}$ ; (c)  $0.2 \text{ mg/mL}$

兹频谱仪接收端接收到的能量进一步减小,测试系统的信噪比降低,灵敏度受到影响。其次,实验过程中

人为操作及环境的变化也给实验结果造成了一定的影响。此外,为了兼顾测试效率与准确性,实验中采用的频率步长为 200 MHz,通过进一步缩短频率步长,有望进一步提升传感器的灵敏度。值得注意的是,已有工作证明,综合考察超材料透射率和共振频率的偏移情况,可提高禽流感病毒种类鉴别的准确性<sup>[24]</sup>。可见,优化实验环境,结合待测物引起的超材

料透射率及共振峰的变化情况,缩短频率步长,可进一步提高检测灵敏度,实现对更低浓度待测物的检测,并赋予传感器特异性。此外,值得注意的是,所述的超材料由不溶于丙酮、乙醇的硅及金属铝构成,且实际检测流程中的烘干等过程不会对超材料自身材料、结构造成影响,因此结合清洗步骤后,超材料具备重复利用性。

表 2 不同待测物体积质量下的共振频率及频率偏移量

Table 2 Resonance frequencies and frequency offsets under different volume mass values of determinands

Volume mass / (mg·mL <sup>-1</sup> )	Resonance peak without determinand /GHz	Resonance peak with determinand /GHz	$\Delta f$ /GHz
1.0	800.8577	798.8537	2.0040
0.3	800.1836	799.3107	0.8729
0.2	801.6216	801.5831	0.0385

## 4 结 论

基于超材料与太赫兹光谱技术构建了生物大分子(牛血清白蛋白)的高效传感器。实验结果表明,待测物的加入能够引起太赫兹透射光谱显著的偏移,传感器谐振频率的变化量随待测物浓度的增大而增大。当牛血清白蛋白溶液的体积质量在 2~8 mg/mL 范围内时,谱线偏移量与体积质量呈线性相关性,展现出所提出的传感器检测物质浓度的潜力。此外,该传感器的最低浓度检测限可以达到 0.3 mg/mL。综上,所构建的牛血清白蛋白传感器具有灵敏度高、操作简单、高效等优点。后续通过进一步优化超材料参数,综合利用共振峰的位置与幅度信息,改善测试环境,有望获得具有特异性、灵敏度更高的生物大分子传感器。

**致谢** 感谢中国科学院上海光学精密机械研究所朱菁副研究员、廖洋副研究员、张佩高级工程师及中国科学院上海免疫与感染研究所胡轶红副研究员在实验过程中提供的帮助。

## 参 考 文 献

- [1] Yang K, Li J N, Lamy de la Chapelle M, et al. A terahertz metamaterial biosensor for sensitive detection of microRNAs based on gold-nanoparticles and strand displacement amplification[J]. *Biosensors and Bioelectronics*, 2021, 175: 112874.
- [2] 田野, 郭丝霖, 曾雨珊, 等. 强场太赫兹光源及其物质调控研究(特邀)[J]. *光子学报*, 2020, 49(11): 1149001.  
Tian Y, Guo S L, Zeng Y S, et al. High-field terahertz sources and matter manipulation(invited)[J]. *Acta Photonica Sinica*, 2020, 49(11): 1149001.
- [3] 余琦, 蒋玲, 章龙, 等. 氨基酸的太赫兹光谱研究进展[J]. *红外技术*, 2018, 40(3): 220-226.  
Yu Q, Jiang L, Zhang L, et al. Research progress of THz spectroscopy of amino acids[J]. *Infrared Technology*, 2018, 40(3): 220-226.
- [4] Walther M, Fischer B M, Uhd Jepsen P. Noncovalent intermolecular forces in polycrystalline and amorphous saccharides in the far infrared[J]. *Chemical Physics*, 2003, 288(2/3): 261-268.
- [5] Walther M, Plochocka P, Fischer B, et al. Collective vibrational modes in biological molecules investigated by terahertz time-domain spectroscopy[J]. *Biopolymers*, 2002, 67(4/5): 310-313.
- [6] Cao C, Serita K, Kitagishi K, et al. Terahertz spectroscopy tracks proteolysis by a joint analysis of absorbance and Debye model[J]. *Biophysical Journal*, 2020, 119(12): 2469-2482.
- [7] 王玥, 崔子健, 张晓菊, 等. 超材料赋能先进太赫兹生物化学传感检测技术的研究进展[J]. *物理学报*, 2021, 70(24): 247802.  
Wang Y, Cui Z J, Zhang X J, et al. Research progress of metamaterials powered advanced terahertz biochemical sensing detection techniques[J]. *Acta Physica Sinica*, 2021, 70(24): 247802.
- [8] Yoneyama H, Yamashita M, Kasai S, et al. Terahertz spectroscopy of native-conformation and thermally denatured bovine serum albumin (BSA)[J]. *Physics in Medicine and Biology*, 2008, 53(13): 3543-3549.
- [9] Yoneyama H, Yamashita M, Kasai S, et al. Membrane device for holding biomolecule samples for terahertz spectroscopy[J]. *Optics Communications*, 2008, 281(7): 1909-1913.
- [10] Cheon H, Yang H J, Lee S H, et al. Terahertz molecular resonance of cancer DNA[J]. *Scientific Reports*, 2016, 6: 37103.
- [11] Han X H, Yan S H, Zang Z Y, et al. Label-free protein detection using terahertz time-domain spectroscopy[J]. *Biomedical Optics Express*, 2018, 9(3): 994-1005.
- [12] Pendry J B. Negative refraction makes a perfect lens[J]. *Physical Review Letters*, 2000, 85(18): 3966-3969.
- [13] Grady N K, Heyes J E, Chowdhury D R, et al. Terahertz metamaterials for linear polarization conversion and anomalous refraction[J]. *Science*, 2013, 340(6138): 1304-1307.
- [14] Cong L Q, Tan S Y, Yahiaoui R, et al. Experimental demonstration of ultrasensitive sensing with terahertz metamaterial absorbers: a comparison with the metasurfaces[J]. *Applied Physics Letters*, 2015, 106: 031107.
- [15] Chen M M, Xiao Z Y, Lu X J, et al. Simulation of dynamically tunable and switchable electromagnetically induced transparency analogue based on metal-graphene hybrid metamaterial[J]. *Carbon*, 2020, 159: 273-282.
- [16] Zhang J, Mu N, Liu L H, et al. Highly sensitive detection of malignant glioma cells using metamaterial-inspired THz biosensor based on electromagnetically induced transparency[J]. *Biosensors and Bioelectronics*, 2021, 185: 113241.
- [17] Hähnel D, Golla C, Albert M, et al. A multi-mode super-Fano mechanism for enhanced third harmonic generation in silicon metasurfaces[J]. *Light: Science & Applications*, 2023, 12: 97.
- [18] Yue L S, Wang Y, Cui Z J, et al. Multi-band terahertz resonant absorption based on an all-dielectric grating metasurface for chlorpyrifos sensing[J]. *Optics Express*, 2021, 29(9): 13563-13575.
- [19] Yang Y P, Xu D Q, Zhang W L. High-sensitivity and label-free identification of a transgenic genome using a terahertz meta-

- biosensor[J]. *Optics Express*, 2018, 26(24): 31589-31598.
- [20] 王庆芳, 王泽云, 韩超, 等. 基于太赫兹超材料芯片的生物混合物定量检测研究[J]. *中国激光*, 2021, 48(23): 2314001.
- Wang Q F, Wang Z Y, Han C, et al. Quantitative detection of biological mixtures based on terahertz metamaterial chip[J]. *Chinese Journal of Lasers*, 2021, 48(23): 2314001.
- [21] Lin S J, Xu X L, Hu F R, et al. Using antibody modified terahertz metamaterial biosensor to detect concentration of carcinoembryonic antigen[J]. *IEEE Journal of Selected Topics in Quantum Electronics*, 2021, 27(4): 6900207.
- [22] Li Y Y, Chen X Y, Hu F R, et al. Four resonators based high sensitive terahertz metamaterial biosensor used for measuring concentration of protein[J]. *Journal of Physics D: Applied Physics*, 2019, 52(9): 095105.
- [23] Keshavarz A, Vafapour Z. Sensing avian influenza viruses using terahertz metamaterial reflector[J]. *IEEE Sensors Journal*, 2019, 19(13): 5161-5166.
- [24] Park S J, Cha S H, Shin G A, et al. Sensing viruses using terahertz nano-gap metamaterials[J]. *Biomedical Optics Express*, 2017, 8(8): 3551-3558.
- [25] Lee D K, Kang J H, Kwon J, et al. Nano metamaterials for ultrasensitive terahertz biosensing[J]. *Scientific Reports*, 2017, 7: 8146.
- [26] Chan J F W, Yip C C Y, To K K W, et al. Improved molecular diagnosis of COVID-19 by the novel, highly sensitive and specific COVID-19-RdRp/Hel real-time reverse transcription-PCR assay validated *in vitro* and with clinical specimens[J]. *Journal of Clinical Microbiology*, 2020, 58(5): e00310-e00320.
- [27] Guo L, Ren L L, Yang S Y, et al. Profiling early humoral response to diagnose novel coronavirus disease (COVID-19) [J]. *Clinical Infectious Diseases*, 2020, 71(15): 778-785.
- [28] Noor Z, Ahn S B, Baker M S, et al. Mass spectrometry-based protein identification in proteomics—a review[J]. *Briefings in Bioinformatics*, 2021, 22(2): 1620-1638.
- [29] Sengupta R, Khand H, Sarusi G. Terahertz impedance spectroscopy of biological nanoparticles by a resonant metamaterial chip for breathalyzer-based COVID-19 prompt tests[J]. *ACS Applied Nano Materials*, 2022, 5(4): 5803-5812.

## Research of Bovine Serum Albumin Sensor Based on Terahertz Metamaterials

Zheng Zhuorui<sup>1,4</sup>, Zhong Hui<sup>\*</sup>, Nie Yongxiao<sup>1,2</sup>, Lin Ting<sup>1,3</sup>, Fang Yifei<sup>1</sup>,  
Song Liwei<sup>1,4</sup>, Tian Ye<sup>1,4</sup>

<sup>1</sup>State Key Laboratory of High Field Laser Physics, Shanghai Institute of Optics and Fine Mechanics, Chinese Academy of Sciences, Shanghai 201800, China;

<sup>2</sup>School of Optical and Electronic Information, Huazhong University of Science and Technology, Wuhan 430074, Hubei, China;

<sup>3</sup>College of Optical-Electrical and Computer Engineering, University of Shanghai for Science and Technology, Shanghai 200093, China;

<sup>4</sup>Center of Materials Science and Optoelectronics Engineering, University of Chinese Academy of Sciences, Beijing 100049, China

### Abstract

**Objective** Terahertz waves are electromagnetic waves with frequencies of 0.1–10.0 THz. They have the characteristics of wide bandwidth, strong penetration, and low photon energy. Notably, the energy levels of the terahertz spectrum correspond to the rotational and vibrational energy levels of several biological macromolecules. Therefore, the terahertz spectroscopy technology can be used to study the properties of biomolecules, such as their molecular structures and their molecular interactions with the surrounding environment. Because the wavelength of a terahertz wave (0.03–3.00 mm) is not in the same order of magnitude as the characteristic size of common biological macromolecules, it is difficult to produce sufficient interaction between the trace levels of biological macromolecules contained in the sample and the terahertz wave, and the weak change in the terahertz spectral line is difficult to capture. Metamaterial is an artificial material whose electromagnetic properties can be manipulated artificially. By combining terahertz spectroscopy technology with metamaterials, the small disturbance to the metamaterial caused by trace-level objects can result in significant changes in the spectra of metamaterials, and thus make high-sensitivity detection of biomacromolecules possible. In this study, a resonant terahertz metamaterial is used to enhance the interaction between terahertz wave and the determinand, and a bovine serum albumin (BSA) solution is selected as the analyte. An efficient BSA sensor is constructed using terahertz spectroscopy technology. The relationship between the concentration of the BSA solution and the resonance frequency offset of the sensor is analyzed, and the limit of detection of the sensor is examined.

**Methods** To achieve rapid and highly sensitive detection of BSA solution, the unit structure designed by Sengupta *et al.* is adopted. Because of the C<sub>4</sub> symmetry of the structure, the metamaterial-based sensor is insensitive to polarization. The electromagnetic properties of the metamaterial are simulated by full-wave numerical simulation. According to the simulation results, the above structure has resonance absorption near 0.8 THz. When the refractive index of the material at the surface of the metamaterial changes, the resonance frequency of the metamaterial shifts. By combining the terahertz spectrum technology, the relationship between the resonance frequency shift of the metamaterial and the concentration of determinand is established. The

schematic of the experimental setup is shown in Fig. 1. First, the transmission spectrum of the metamaterial without a determinand is measured with a terahertz spectrometer and used as the background. Second, quantitative BSA is dissolved in distilled water to prepare a certain concentration of BSA solution, and the 20  $\mu\text{L}$  solution is collected through a microsampler and dropped onto the metamaterial. The metamaterial is heated at 70  $^{\circ}\text{C}$  for 10 min. The transmission spectra of the metamaterials are measured using a terahertz spectrometer to provide a sample group. During the experiment, to reduce error, the linear weighted average processing is carried out on the data of the adjacent points in a single scanning. The final data for each sample is the average of the three scanning results. A second-order Gaussian fitting method is used to fit the transmission spectral data of the background and sample groups nonlinearly, and the resonance frequency shift of the metamaterial is obtained by comparing the fitted curves.

**Results and Discussions** A resonance absorption peak of approximately 0.8 THz for the metamaterial without a determinand is found (Fig. 2). According to the fitting curves, a BSA solution with a volume mass of 2 mg/mL can induce a 10.43-GHz redshift in the resonant frequency of the metamaterial. Using the control variable method, several groups of solutions with different volume mass values (2, 3, 4, and 8 mg/mL) are configured, and their terahertz transmission spectra are measured and compared with the transmission spectrum of the bare metamaterial (Fig. 3). With a gradual increase in the concentration of the determinand, the resonance frequency of the metamaterial gradually moves in the lower frequency direction (Table 1). When the solution volume mass is in the range of 2–8 mg/mL, a linear relationship exists between the resonance frequency shift of the metamaterial and the volume mass of the determinand (Fig. 4). The concentration of the BSA solution is determined according to a linear relationship. When the concentration of the BSA solution is reduced continuously and when the volume mass is decreased to 0.3 mg/mL, the frequency offset of the resonance chip is 0.87 GHz. When the volume mass is further decreased to 0.2 mg/mL, the resonance shift is less than 0.04 GHz, which is significantly lower than the sampling step size of the spectrometer (Fig. 5 and Table 2). Furthermore, 0.3 mg/mL exhibits the lowest detection limit. By optimizing the experimental environment, considering the change in transmittance and resonance frequency, and shortening the frequency step size, the detection sensitivity can be further improved, the limit of detection can be reduced, and the sensor specificity can be enhanced.

**Conclusions** Based on metamaterials and terahertz spectroscopy, an efficient sensor for biological macromolecules is constructed. The experimental results show that the addition of determinand can cause a significant shift in the terahertz transmission spectrum and the variation in the resonant frequency of the sensor increases with an increase in the concentration of the determinand. When the volume mass of the BSA solution is in the range of 2–8 mg/mL, the offset of the resonant frequency is linearly correlated with the volume mass, demonstrating the potential of the proposed sensor for detecting the substance concentration. In addition, the limit of detection is 0.3 mg/mL. In conclusion, the proposed BSA sensor has high sensitivity, simple operation, and high efficiency. Subsequently, by further optimizing the materials and parameters of metamaterials, comprehensively utilizing the position and amplitude information of the resonance peak, and improving the test environment, it should be possible to obtain biological macromolecule sensors with higher specificity and sensitivity.

**Key words** spectroscopy; terahertz; metamaterial; bovine serum albumin; sensor